Results in Control and Optimization 22 (2026) 100653

Contents lists available at ScienceDirect

Results in Control and Optimization

journal homepage: www.elsevier.com/locate/rico

Recursive feasibility without terminal constraints via parent–child MPC architecture

Filip Surma *, Anahita Jamshidnejad

Delft University of Technology, Kluyverweg 1, Delft, 2629 HS, South Holland, The Netherlands

ARTICLE INFO

Keywords:
Model predictive control
Hierarchical control
Robust tube-based model predictive control
Computational efficiency

ABSTRACT

This paper introduces a novel hierarchical model predictive control (MPC) framework, called the Parent–Child MPC architecture, designed to ensure recursive feasibility without relying on terminal constraints. The proposed architecture targets nonlinear constrained systems with Lipschitz continuous dynamics, such as quadrotors, helicopters and autonomous bicycles. For such systems, traditional MPC approaches may suffer from computational intractability or conservativeness due to needing terminal constraints. The proposed framework couples a small-horizon, high-fidelity Child MPC with one or more large-horizon, simplified Parent MPC layers. The Parent layers provide robust invariant tubes that replace terminal constraints, enabling scalable planning and stability guarantees. Two case studies, including a linear double integrator system and a nonlinear system, demonstrate the effectiveness of the architecture. Compared to standard robust tube-based MPC, the Parent–Child MPC achieves up to an eight-fold reduction in solver time and a three-fold increase in controllable prediction horizon. It also maintains performance within 3% of robust tube-based MPC. These results highlight the potential of this architecture for real-time control of complex, nonlinear systems under uncertainty.

1. Introduction

Model predictive control (MPC) employs a model of the system to predict its future behavior over a finite time horizon and to accordingly optimize the control input trajectory. A key strength of MPC is its ability to explicitly incorporate constraints during the optimization procedure [1].

As infinite constrained optimization is usually computationally intractable, MPC operates over a finite prediction horizon. Due to this, ensuring stability for MPC is generally challenging, and is commonly achieved via, e.g., enforcing passivity conditions [2], using the augmented stage cost function corresponding to a single time step as a control Lyapunov function [3], or treating the optimal cost of the MPC optimization problem as a control Lyapunov function and demonstrating its decline [1].

These methods for MPC often involve supplementary, terminal constraints. Applied exclusively to the final predicted state, terminal constraints guide the system towards a terminal state region $\mathcal{X}^{\mathrm{f}} \subseteq \mathcal{X}$ near its destination (with $\mathcal{X}$ the admissible state set). The N-step controllable set $\mathcal{X}_N$ set is a set including all states that are steerable by an admissible control input sequence of length N – the number of time steps across the prediction horizon – into set $\mathcal{X}^{\mathrm{f}}$ [4]. For larger prediction horizons, this controllable set is usually expanded. In other words, some states, although safely steerable into $\mathcal{X}^{\mathrm{f}}$ with large prediction horizons, lie outside the reach of short-horizon MPC.

Large-horizon MPC is typically computationally prohibitive [5]. It is thus common to simplify (e.g., linearize) the prediction model [6]. This, however, potentially leads to constraint violations, due to model inaccuracies. Alternatively, as explained in [7],

* Corresponding author.
E-mail addresses: f.surma@tudelft.nl (F. Surma), a.jamshidnejad@tudelft.nl (A. Jamshidnejad).

https://doi.org/10.1016/j.rico.2025.100653
Received 19 June 2025; Received in revised form 25 December 2025; Accepted 29 December 2025
Available online 30 December 2025

the sampling time is manipulated to enlarge the controllable state set without increasing the prediction horizon. The main objective of this paper is to propose an architecture that extends single-level MPC to multi-level MPC, in order to reduce the required computations while maintaining robustness and performance.

Beyond MPC, recent advances in alternative control paradigms have been reported, including deterministic artificial intelligence approaches [8], robotics-oriented methods for center-of-mass estimation and trajectory shaping [9], and bio-inspired or adaptive controllers [10]. These contributions illustrate the diversity of modern control research. Nevertheless, MPC remains unique in systematically handling multi-objective optimization with hard state and input constraints. This motivates the present focus on advancing MPC methodologies. The proposed Parent–Child MPC architecture should be viewed as complementary to these recent advances.

Combined approaches integrate MPC with other controllers. An example involves dividing the prediction horizon into a control horizon governed by MPC and a segment where the last MPC input is simply repeated [11]. This approach usually enhances computational efficiency by reducing the number of decision variables. Alternatively, after executing the MPC trajectory for given time steps, a terminal control law (e.g., a linear quadratic regulator for linear systems) is activated [12]. This method is based on invariance of the terminal set.

These strategies all rely on reaching a given terminal set via MPC, without inherently enlarging the N-step controllable state set. Hierarchical MPC offers promising alternatives. Numerous hierarchical MPC schemes have been proposed in the literature, though not all of them focus on reducing the optimization time. For example, [13] employs a hierarchical approach to decompose the control problem into path planning and path following. In [14], MPC performs high-level planning to generate optimal reference trajectories, while a lower-level controller executes the plan. However, this methodology does not employ MPC (or another optimal controller) at the lowest layer, which may result in suboptimal performance. Similarly, in [15] a hierarchical MPC architecture is proposed for complex building energy systems, but without demonstrating stability guarantees. In [16], a stable and robust hierarchical MPC was proposed. Nevertheless, in all these approaches, the higher-level controller attempts to identify an optimal trajectory, while the lower-level controller is limited to tracking it. In contrast, our approach assigns full optimal decision-making authority to the lower-level controller, granting it full knowledge of the objective and freedom in achieving it, while the higher-level controller ensures safety and stabilizes the system by imposing additional constraints.

A recent bi-level MPC architecture in [17] synergizes two MPC formulations: ‘‘Rough long-vision’’ MPC with a coarse prediction model and large sampling time, and ‘‘detailed short-vision’’ MPC for enhancing and executing the plan across a smaller prediction horizon with smaller sampling times. Long-term MPC provides a trajectory that guides the constraints of short-term MPC. This architecture has been extended to long-term exploration planning for multi-robot systems in [18], with highly promising results, but no formal stability guarantees.

Inspired by this, the challenge of reaching a designated terminal set through online decision-making is addressed by proposing a multi-level architecture composed of interconnected MPC systems, leveraging robust Tube-based MPC (TMPC). TMPC ensures constraint satisfaction under bounded uncertainties without significantly increasing online computational complexity [1]. It uses a fixed-shape tube (e.g., a polyhedron or ellipsoid [19]) around the nominal trajectory to guarantee safety [20]. The nominal component of TMPC governs the center of the tube, while an ancillary controller maintains the actual state within the tube. The fixed tube structure, however, may lead to conservative behavior and reduced performance. For instance, applied to a wheeled E-puck robot [21], TMPC caused a substantial unnecessary reduction in the robot velocity, up to 30% [22]. This performance degradation stems from the dual role of the ancillary control law, as it should both ensure stability and compensate for disturbances and model discrepancies. These dual objectives restrict the flexibility of nominal MPC in selecting optimal control inputs.

Key contributions of the paper are:

- A novel hierarchical control framework, called the Parent–Child MPC architecture, is introduced. The framework effectively replaces the nominal component in TMPC for certain nonlinear systems. It guarantees convergence to a designated terminal set without imposing a terminal constraint, thereby avoiding conservativeness and risk of infeasibility typically associated with such constraints.
- A small-horizon Child MPC (C-MPC) controller directly steers the system, emphasizing local optimality. One or more large-horizon Parent MPC (P-MPC) layers address stability and long-term feasibility. Strategic interactions of these layers allow to replace terminal constraints with adjustable stage-wise state constraints, including robust positive invariant tubes derived by Parent layers. This significantly enlarges the feasible exploration space of C-MPC, leading to improved performance.
- The cross section of these tubes is composed of a fixed subset $\mathcal{E}^{\mathrm{P}}$ of the state space. It is proven that $\mathcal{E}^{\mathrm{P}}$ is also a robust positive invariant set for the C-MPC nominal trajectory. Once this nominal trajectory enters $\mathcal{E}^{\mathrm{P}}$, the goal of Parent–Child MPC architecture is met, allowing a secondary low-complexity controller (e.g., small-horizon conventional TMPC) to steer the actual state towards a neighborhood of the origin.

Similarly to [17], the trajectories of P-MPC layers – based on linear TMPC [20] — are used to formulate constraints for C-MPC that ensure long-term feasibility and stability. C-MPC, similarly to an ancillary controller, directly steers the system, which is initialized far from its desired state, with no reference trajectory. Unlike the approach in [23], where MPC serves as an ancillary controller within a nonlinear TMPC framework, C-MPC does not track the nominal trajectories of P-MPC. Instead, it shares the same cost function as P-MPC, while employing a more accurate prediction model and finer sampling times. The results presented in this paper are primarily intended for practitioners seeking to implement MPC in scenarios where, despite strong theoretical justification (e.g. the presence of hard constraints or highly accurate models), the computational burden hinders or prevents practical deployment. In such

cases, the proposed architecture offers a viable solution by significantly reducing computational effort, while preserving stability and robustness, with only a minor loss in optimality.

Section 2 formulates the problem. Section 3 details the Parent–Child MPC architecture. Section 4 presents and discusses the results of a case study, and Section 5 concludes the paper and proposes directions for future research. Moreover, abbreviations and mathematical notations used frequently in the paper have been included together with their explanations and definitions in two tables in Appendix A and Appendix B, respectively.

2. Problem formulation

This section describes the problem of controlling a nonlinear system subject to additive disturbances, with the goal of steering the system from an arbitrary initial state to a desired target state. The system model follows the formulation in [24].

2.1. System modeling

The system dynamics is described in discrete time by the following nonlinear model subject to additive disturbances:

$$\boldsymbol{x}_{k+1} = A\boldsymbol{x}_k + g(\boldsymbol{x}_k) + B\boldsymbol{u}_k + \boldsymbol{w}_k \tag{1}$$

where $\boldsymbol{x}_k \in \mathbb{R}^n \subseteq \mathcal{X}$ is the state vector, $\boldsymbol{u}_k \in \mathbb{R}^m \subseteq \mathcal{U}$ is the control input vector, $\boldsymbol{w}_k \in \mathbb{R}^n \subseteq \mathcal{W}$ is an unknown bounded disturbance vector. The states, control inputs, and disturbances are constrained to convex, compact sets $\mathcal{X}$, $\mathcal{U}$, and $\mathcal{W}$, respectively. Function $g(\cdot)$ is nonlinear Lipschitz with Lipschitz constant $L > 0$, satisfying $g(\mathbf{0}) = \mathbf{0}$. The matrix pair (A, B) is stabilizable. Lipschitz continuity of $g(\cdot)$ implies that:

$$\left\|g(\boldsymbol{x}_1) - g(\boldsymbol{x}_2)\right\| \leq L \left\|\boldsymbol{x}_1 - \boldsymbol{x}_2\right\| \qquad \forall \boldsymbol{x}_1, \boldsymbol{x}_2 \in \mathcal{X} \tag{2}$$

Note that the assumptions considered on function $g(\cdot)$ are standard in the relevant literature. More specifically, $g(\mathbf{0}) = \mathbf{0}$ ensures that the system admits an equilibrium. Systems without an equilibrium cannot be directly controlled by MPC-based methods, including TMPC. Moreover, Lipschitz continuity is a standard assumption in various works on systematic control of nonlinear systems via MPC; while a large Lipschitz constant enlarges the tube, unlike conventional TMPC, our framework does not require minimizing this tube size – as is detailed later in Section 3.1.2 – making the approach less conservative.

2.2. Control problem

The control objective is to regulate the state towards a suitable robust positive invariant set including the origin, as defined in [20]. Until this goal is reached, a stage cost $l(\cdot,\cdot)$, given below, is accumulated, with Q and R positive definite matrices:

$$l(\boldsymbol{x}_k, \boldsymbol{u}_k) = \boldsymbol{x}_k^\top Q \boldsymbol{x}_k + \boldsymbol{u}_k^\top R \boldsymbol{u}_k \tag{3}$$

As shown in [25], systems given by (1) under the stated conditions, can robustly be controlled using TMPC. The nominal optimization problem of nonlinear TMPC at time step k, with prediction horizon N, for system (1) is given by:

$$V(\boldsymbol{x}_k) = \min_{\tilde{\boldsymbol{z}}_{k:k+N}, \tilde{\boldsymbol{v}}_{k:k+N-1}} \sum_{i=k}^{k+N-1} \left(\boldsymbol{z}_{i|k}^\top Q\, \boldsymbol{z}_{i|k} + \boldsymbol{v}_{i|k}^\top R\, \boldsymbol{v}_{i|k}\right) + \boldsymbol{z}_{k+N|k}^\top P \boldsymbol{z}_{k+N|k} \tag{4a}$$

such that for $i = k, \ldots, k+N-1$:

$$\boldsymbol{x}_k \in \{\boldsymbol{z}_k\} \oplus \mathcal{E} \tag{4b}$$

$$\boldsymbol{z}_{i+1|k} = A\boldsymbol{z}_{i|k} + g\left(\boldsymbol{z}_{i|k}\right) + B\boldsymbol{v}_{i|k} \tag{4c}$$

$$\boldsymbol{z}_{i+1|k} \in \mathcal{X} \ominus \mathcal{E} \tag{4d}$$

$$\boldsymbol{v}_{i|k} \in \mathcal{V} \tag{4e}$$

$$\boldsymbol{z}_{k+N|k} \in \mathcal{Z}^{\mathrm{f}} \tag{4f}$$

which, rather than directly steering the system state $\boldsymbol{x}_k$, determines nominal control input $\boldsymbol{v}_k$ to steer the nominal state $\boldsymbol{z}_k$. The nominal prediction model is given via (4c), which eliminates the disturbance term $\boldsymbol{w}_k$ from (1). The nominal state trajectory represents the center of a rigid tube with cross section $\mathcal{E}$, i.e., the set of possible errors between nominal and actual states. The state admissibility constraint (4d) has been tightened to ensure the actual state, impacted by uncertainties, remains within the admissible state set $\mathcal{X}$. The notation $a_{k_2|k_1}$, with $k_2 \geq k_1$, shows the value of variable a at time step k_2 predicted at time step k_1, with $a_{k_1|k_1} := a_{k_1}$. Tilde for decision variables shows a sequence, where $\tilde{a}_{k_3:k_4}$ with $k_4 \geq k_3$ represents $[a_{k_3}, \ldots, a_{k_4}]^\top$. Constraint (4b) adjusts the nominal state $\boldsymbol{z}_k$ at time step k to locate the cross section $\{\boldsymbol{z}_k\} \oplus \mathcal{E}$ of the tube within set $\mathcal{X}$, so that the measured state $\boldsymbol{x}_k$ lies within the tube. For all time steps $i = k, \ldots, k+N-1$, the actual control input $\boldsymbol{u}_{i|k}$ should satisfy $\boldsymbol{u}_{i|k} \in \mathcal{U}$. This requires defining tightened constraints on nominal control inputs, as is done in (4e). The terminal constraint (4f), where $\mathcal{Z}^{\mathrm{f}}$ is a control invariant set, designed as a tightened version of the actual terminal state set $\mathcal{X}^{\mathrm{f}}$, together with the terminal cost $\boldsymbol{z}_{k+N|k}^\top P\, \boldsymbol{z}_{k+N|k}$ in (4a), ensures recursive feasibility — i.e., if a solution initially exists, a solution exists for all future time steps. However, as explained earlier,

imposing such a terminal constraint may restrict the set of initial states from which the system is steerable to the origin. Note that $\oplus$ and $\ominus$ show the Minkowski set summation and subtraction, respectively.

The actual system, which is prone to disturbances and model discrepancies, is controlled via an ancillary control law:

$$\boldsymbol{u}_k = \pi(\boldsymbol{x}_k, \boldsymbol{z}_k, \boldsymbol{v}_k), \tag{5}$$

designed to ensure, through the tightened constraint (4d), that the evolved actual state $\boldsymbol{x}_{k+1}$ remains within the tube, provided that the current state $\boldsymbol{x}_k$ satisfies (4b). The tube cross section $\{\boldsymbol{z}_{i|k}\} \oplus \mathcal{E}$, for all time steps $i = k, \dots, k+N-1$, is a robust positive invariant set when the system follows control input $\pi\left(\boldsymbol{x}_k, \boldsymbol{z}_k, \boldsymbol{v}_k\right)$.

The goal is to design an MPC-based control architecture that can steer the system to the origin from any admissible initial state – assuming a feasible control problem – while guaranteeing stability and recursive feasibility. Although solving (4) with a sufficiently large prediction horizon theoretically achieves this goal, the computational burden may be prohibitive [22]. The control architecture proposed in this paper addresses this issue by alternately solving an additional quadratic program alongside the nonlinear program, reducing the computational complexity while maintaining the desired properties.

3. Proposed architecture: Parent-child MPC

This section discusses the proposed Parent–Child MPC architecture, which replaces the nominal problem in conventional TMPC given by (4) to offer a computationally efficient alternative with stability guarantees. The Parent MPC (P-MPC) extends standard linear TMPC, incorporating both a nominal MPC problem and a feedback ancillary control law. In contrast, the Child MPC (C-MPC) leverages the nominal problem from the nonlinear TMPC formulation in (4) to more flexibly steer the system. Unlike traditional TMPC, C-MPC omits terminal constraints, thereby eliminating the restrictive influence of these sets, as discussed in Section 1. Instead, C-MPC operates under additional stage-wise constraints derived by P-MPC, in the form of translated tubes – robust positive invariant sets – composed of a fixed subset $\mathcal{E}^{\mathrm{P}}$ of the state space centered along the Parent nominal state trajectory.

Remark 1. While the proposed architecture eliminates the need for terminal constraints in the C-MPC layer, P-MPC still employs a terminal constraint during long-term planning to ensure feasibility and stability. This distinction highlights that terminal constraints are not universally unnecessary, but are shifted to the higher-level controller in our framework, where their estimation is significantly easier and computationally more tractable.

Set $\mathcal{E}^{\mathrm{P}}$ is designed to lie within the controllable state set, from which the nominal Child trajectory is steerable into a desired terminal set. It is proven that, under the Parent–Child MPC strategy, the untranslated set $\mathcal{E}^{\mathrm{P}}$ itself is a robust positive invariant set for the nominal C-MPC trajectory. Therefore, once the nominal C-MPC trajectory enters this set, the primary objective of the Parent–Child MPC architecture is fulfilled. From this point onward, a secondary control phase – such as a conventional TMPC scheme with a small horizon (and thus affordable online computations), or another control-invariant strategy – may be employed to steer the actual state trajectory towards a desired neighborhood of the origin.

P-MPC employs a simplified nominal version of the system model in (1) that eliminates both the Lipschitz nonlinearity and the additive disturbances. The underlying linear TMPC formulation of P-MPC is designed to mitigate the uncertainties introduced by the model discrepancy that stems from omitting the Lipschitz nonlinearities of the original system. By adopting a coarser sampling time for prediction and optimization, P-MPC reduces computational complexity and supports larger prediction horizons. While this long-term planning facilitates stability, directly following the trajectories generated by P-MPC may lead to suboptimal performance due to model inaccuracies.

C-MPC operates at a finer resolution, using a nominal, yet nonlinear, version of the model in (1) that solely eliminates the additive disturbances. Exploiting its more accurate model, C-MPC focuses on short-term optimality within a disturbance-driven tube, while inheriting stability and feasibility guarantees from P-MPC. An ancillary control strategy (such as the one in [23]) is ultimately employed to reject these disturbances.

The Parent–Child MPC architecture integrates long-term planning capabilities of P-MPC with responsiveness and short-term optimality of C-MPC, while preserving stability and recursive feasibility. The primary distinction between conventional nonlinear TMPC and the Parent–Child MPC architecture lies in the role of the nominal components: In standard TMPC an ancillary controller ensures stability by keeping the state within a tube located in the state space through the nominal controller. Thus, reducing the tube size is essential to enhancing flexibility in the nominal trajectory, thereby improving the performance (see tightened state admissibility constraint (4d)). In contrast, within the Parent–Child MPC architecture, C-MPC enhances the optimality, whereas P-MPC ensures stability and recursive feasibility by generating a suitable modeling error tube. Consequently, enhancing the flexibility of C-MPC and, thus, the system performance, requires an enlarged modeling error tube.

Next, the formulations of P-MPC and C-MPC are presented. The actual state at time step k is denoted by $\boldsymbol{x}_k$, which is guided by the actual control input $\boldsymbol{u}_k$. The nominal state and control input of P-MPC and C-MPC are represented by $\boldsymbol{z}_k^{\mathrm{P}}, \boldsymbol{v}_k^{\mathrm{P}}$ and $\boldsymbol{z}_k^{\mathrm{C}}, \boldsymbol{v}_k^{\mathrm{C}}$, respectively. The prediction horizon and cross section of the tube – a robust positive invariant set for rejecting uncertainties – for P-MPC and C-MPC are N^{P}, $\mathcal{E}^{\mathrm{P}}$ and N^{C}, $\mathcal{E}^{\mathrm{C}}$, respectively. The actual state and input of P-MPC are given by $\boldsymbol{x}_k^{\mathrm{P}}$ and $\boldsymbol{u}_k^{\mathrm{P}}$.

3.1. Parent MPC

The formulation of P-MPC is based on standard linear TMPC [20]. Rejecting the additive disturbances $\boldsymbol{w}_k$ affecting the original system modeled by (1) is delegated to C-MPC. Consequently, external disturbances do not appear in the formulation of P-MPC, which is designed for the following dynamic model:

$$\boldsymbol{x}^{\mathrm{P}}_{k+1} = A\boldsymbol{x}^{\mathrm{P}}_k + B\boldsymbol{u}^{\mathrm{P}}_k + \boldsymbol{w}^{\mathrm{P}}_k \tag{6}$$

with $\boldsymbol{w}^{\mathrm{P}}_k = g\left(\boldsymbol{x}^{\mathrm{P}}_k\right)$, i.e., both the additive disturbance $\boldsymbol{w}_k$ and the nonlinear term $g\left(\boldsymbol{x}^{\mathrm{P}}_k\right)$ as a controllable part of the dynamics are eliminated. Instead, the nonlinear term is treated as a bounded additive disturbance $\boldsymbol{w}^{\mathrm{P}}_k$. Since $g(\cdot)$ is Lipschitz continuous and $g(\mathbf{0}) = \mathbf{0}$, the following holds: $\left\|g\left(\boldsymbol{x}^{\mathrm{P}}_k\right)\right\| \leq L\boldsymbol{x}^{\mathrm{P}}_k$. Given the boundedness of the state space $\mathcal{X}$, this ensures that $g\left(\boldsymbol{x}^{\mathrm{P}}_k\right)$ is also bounded.

The model in (6), therefore, structurally resembles a linear system subject to bounded additive disturbances, consistent with the framework in [20]. The nominal component of P-MPC then follows a disturbance-free version of (6), given by:

$$\boldsymbol{z}^{\mathrm{P}}_{k+1} = A\boldsymbol{z}^{\mathrm{P}}_k + B\boldsymbol{v}^{\mathrm{P}}_k \tag{7}$$

In this context, the error $\boldsymbol{e}^{\mathrm{P}}_k$ between the actual model (6) and the nominal model (7) of P-MPC is defined as:

$$\boldsymbol{e}^{\mathrm{P}}_k := \boldsymbol{x}^{\mathrm{P}}_k - \boldsymbol{z}^{\mathrm{P}}_k \tag{8}$$

The simplified design of P-MPC enables its nominal optimization problem to be cast as a convex or quadratic program, significantly reducing computational complexity.

In linear TMPC, the nominal control input is augmented with an ancillary control law in the form of linear state error feedback for regulating the modeling error $\boldsymbol{e}^{\mathrm{P}}_k$. Accordingly, the control input in P-MPC is defined as:

$$\boldsymbol{u}^{\mathrm{P}}_k = \boldsymbol{v}^{\mathrm{P}}_k + K^{\mathrm{P}}\boldsymbol{e}^{\mathrm{P}}_k \tag{9}$$

where K^{P} is a feedback gain matrix selected such that $A + BK^{\mathrm{P}}$ is stable (i.e., all eigenvalues lie strictly within the unit circle). In general, matrix K^{P} is not unique.

The control law in (9) is not directly applied to the actual system. Instead, as is detailed in Section 3.2, it serves as a baseline input around which the nominal C-MPC policy is constructed, and warm-starts the C-MPC nominal optimization. Moreover, at the P-MPC level, the choice of the feedback gain matrix K^{P} is primarily important for the construction of the modeling error tube with cross section $\mathcal{E}^{\mathrm{P}}$. This tube is subsequently injected into C-MPC as a sequence of stage-wise constraints on its nominal state, omitting the need for explicit terminal sets. This tube additionally plays a central role in establishing the recursive feasibility for the Parent–Child MPC architecture.

3.1.1. Nominal problem of P-MPC

The nominal optimization problem of P-MPC spans the Parent prediction horizon N^{P}, and incorporates both the Parent tube with cross section $\mathcal{E}^{\mathrm{P}}$ and the Child tube with cross section $\mathcal{E}^{\mathrm{C}}$.

This optimization problem at time step k is given by:

$$\begin{aligned} &V^{\mathrm{P}}\left(\boldsymbol{z}^{\mathrm{C}}_{k|k-1}\right) \\ &= \min_{\bar{\boldsymbol{z}}^{\mathrm{P}}_{k:k+N^{\mathrm{P}}}, \bar{\boldsymbol{v}}^{\mathrm{P}}_{k:k+N^{\mathrm{P}}-1}} \left\{ \sum_{i=k}^{k+N^{\mathrm{P}}-1} \left({\boldsymbol{z}^{\mathrm{P}}_{i|k}}^{\top} Q\, \boldsymbol{z}^{\mathrm{P}}_{i|k} + {\boldsymbol{v}^{\mathrm{P}}_{i|k}}^{\top} R\, \boldsymbol{v}^{\mathrm{P}}_{i|k} \right) \right. \\ &\quad \left. + {\boldsymbol{z}^{\mathrm{P}}_{k+N^{\mathrm{P}}|k}}^{\top} P\, \boldsymbol{z}^{\mathrm{P}}_{k+N^{\mathrm{P}}|k} \right\} \end{aligned} \tag{10a}$$

such that for $i = k, \ldots, k + N^{\mathrm{P}} - 1$:

$$\boldsymbol{z}^{\mathrm{C}}_{k|k-1} \in \left\{\boldsymbol{z}^{\mathrm{P}}_k\right\} \oplus \mathcal{E}^{\mathrm{P}} \tag{10b}$$

$$\boldsymbol{z}^{\mathrm{P}}_{i+1|k} = A\boldsymbol{z}^{\mathrm{P}}_{i|k} + B\boldsymbol{v}^{\mathrm{P}}_{i|k} \tag{10c}$$

$$\boldsymbol{z}^{\mathrm{P}}_{i+1|k} \in \left(\mathcal{X} \ominus \mathcal{E}^{\mathrm{C}}\right) \ominus \mathcal{E}^{\mathrm{P}} \tag{10d}$$

$$\boldsymbol{v}^{\mathrm{P}}_{i|k} \in \mathcal{V}^{\mathrm{C}} \ominus K^{\mathrm{P}}\mathcal{E}^{\mathrm{P}} \tag{10e}$$

$$\boldsymbol{z}^{\mathrm{P}}_{k+N^{\mathrm{P}}|k} \in \mathcal{Z}^{\mathrm{f,P}} \tag{10f}$$

This problem formulation enhances flexibility by encoding the initial Parent nominal state $\boldsymbol{z}^{\mathrm{P}}_k$ as a decision variable. As enforced by constraint (10b), this state should be determined such that the most recent estimate $\boldsymbol{z}^{C}_{k|k-1}$ of the Child nominal state for time step k lies within the current Parent tube. Since the Parent tube is by design a robust positive invariant set, all future Parent nominal states are then guaranteed to remain within this tube. Note that the nominal Child state $\boldsymbol{z}^{\mathrm{C}}_k$ is a decision variable in C-MPC (see Section 3.2), which is solved only after the P-MPC optimization problem. This explains deploying the most recent available estimation $\boldsymbol{z}^{\mathrm{C}}_{k|k-1}$ as a proxy for the Child nominal state at time step k in constraint (10).

The evolution of the nominal state in P-MPC is governed by the simplified dynamics (7), restated in constraint (10c).

To ensure constraint satisfaction despite model simplifications, constraints (10d) and (10e) impose tightened bounds on state and control input trajectories, respectively. While the trajectories generated by P-MPC do not directly steer the actual system, they indirectly influence the actual trajectories by steering the nominal state trajectory of C-MPC (i.e., the center of the Child tube) to ensure it remains stage-wise within the Parent tube. This condition, as detailed in Section 3.2, is essential to eliminating terminal constraints from the C-MPC formulation. Moreover, C-MPC relies on a simplified model of the system that excludes the additive disturbances. This implies that constraint tightening is necessary to always guarantee state admissibility. Accordingly, as encoded in constraint (10d), the admissible state set $\mathcal{X}$ is first shrunk by the shape of set $\mathcal{E}^{\mathrm{C}}$ — cross section of the disturbance-driven tube of C-MPC — and is further eroded by set $\mathcal{E}^{\mathrm{P}}$ — cross section of the modeling error tube. This ensures that the set $\left\{ \boldsymbol{z}^{\mathrm{P}}_{i|k} \right\} \oplus \mathcal{E}^{\mathrm{P}} \oplus \mathcal{E}^{\mathrm{C}}$, which contains the actual state trajectory for all $i = k, \dots, k + N^{\mathrm{P}} - 1$, remains a subset of admissible set $\mathcal{X}$. A similar tightening is applied to the nominal control inputs of P-MPC. In constraint (10e), the admissible control input set $\mathcal{U}$ is replaced by a tightened set $\mathcal{V}^{\mathrm{C}}$, designed based on the actual control input policy of C-MPC for admissibility of its nominal control inputs (see [23] for details), and is further eroded by the set $K^{\mathrm{P}}\mathcal{E}^{\mathrm{P}}$, thereby reserving room for augmenting the Parent ancillary control law later.

To ensure stability, the terminal state $\boldsymbol{z}^{\mathrm{P}}_{k+N^{\mathrm{P}}|k}$ in P-MPC must lie within a terminal set $\mathcal{Z}^{\mathrm{f,P}}$, enforced via constraint (10f). The associated terminal cost $\boldsymbol{z}^{\mathrm{P}\top}_{k+N^{\mathrm{P}}|k} P\, \boldsymbol{z}^{\mathrm{P}}_{k+N^{\mathrm{P}}|k}$ is defined in quadratic form, with matrix P a constant, positive definite matrix obtained by solving the following discrete-time Lyapunov equation:

$$\left(A + BK^{\mathrm{f,P}}\right)^{\top} P \left(A + BK^{\mathrm{f,P}}\right) + Q + K^{\mathrm{f,P}\top} R K^{\mathrm{f,P}} = P \tag{11}$$

Matrices $A, B, K^{\mathrm{f,P}}$ define the closed-loop dynamics under a terminal control law that follows a state feedback policy with gain $K^{\mathrm{f,P}}$, while Q and R are the stage cost matrices. Note that the feedback gains K^{P}, used in (9) for the ancillary control law of P-MPC, and $K^{\mathrm{f,P}}$, used to determine the terminal cost, both need to stabilize the simplified nominal model (7). However, they do not necessarily need to be identical. Their independent design can introduce flexibility, as gain K^{P} influences the shape and size of $\mathcal{E}^{\mathrm{P}}$, i.e., the modeling error set, which constrains the nominal trajectory of C-MPC, while gain $K^{\mathrm{f,P}}$ affects the size of the terminal set $\mathcal{Z}^{\mathrm{f,P}}$ for P-MPC, which determines the admissible endpoint of the nominal trajectory of P-MPC. This terminal set may be defined as a level set of the terminal cost, often taking the form of a polyhedron or an ellipsoid, and obtained by imposing $\boldsymbol{z}^{\mathrm{P}\top}_{k+N^{\mathrm{P}}|k} P\, \boldsymbol{z}^{\mathrm{P}}_{k+N^{\mathrm{P}}|k} < c$, where $c > 0$ is a scalar that determines the size of the terminal set.

3.1.2. Designing the modeling error tube cross section $\mathcal{E}^{P}$

The modeling error tube in P-MPC should be a robust positive invariant set with cross section $\mathcal{E}^{\mathrm{P}}$, such that $\boldsymbol{e}^{\mathrm{P}}_{k} \in \mathcal{E}^{\mathrm{P}}$ implies $\boldsymbol{e}^{\mathrm{P}}_{i} \in \mathcal{E}^{\mathrm{P}}$, for $i > k$. Various state-of-the-art algorithms, e.g., in [19,26], are available for designing cross section of such sets, taking into account that this set is not necessarily unique for a given system subject to given disturbance bounds.

In conventional TMPC, determining optimal shape and size for the tube entails a fundamental trade-off. Smaller tubes, on the one hand, increase flexibility in designing the nominal trajectory by enlarging the tightened state admissible set (see constraints (4d) and (10d)). On the other hand, a smaller tube often necessitates a larger feedback gain matrix K^{P} to ensure robust stability. This, in turn, tightens the admissible control input space (see (10e)). Thus, either design choice may lead to an overall degradation of closed-loop performance.

Since the tube of P-MPC encapsulates the nominal state trajectory of C-MPC, shrinking this tube – while expanding the admissible state space for the nominal state trajectory of P-MPC – has the opposite effect on the nominal state trajectory of C-MPC. The trajectory of C-MPC, however, should enhance optimality. Hence, increased flexibility in state space exploration is highly desirable. Accordingly, the Parent–Child MPC architecture pursues a fundamentally different design objective than that of conventional TMPC: It enlarges the cross section $\mathcal{E}^{\mathrm{P}}$ of the modeling error tube, provided that the computational demand remains tractable for solving the online optimization of C-MPC. Since, by the end of the primary control phase, the nominal C-MPC trajectory lies within set $\mathcal{E}^{\mathrm{P}}$, this set becomes the feasible exploration region for the conventional TMPC in the secondary phase of control. Therefore, the design trade-offs for set $\mathcal{E}^{\mathrm{P}}$ should also account for the computational demands of the conventional TMPC. In practice, for many systems described by (1), with reasonably simple terminal sets, if C-MPC (which operates under stricter constraints) is computationally affordable over horizon N^{C}, then so is the conventional TMPC.

The enlarged tube of P-MPC serves as a stage-wise constraint for C-MPC, thereby expanding its feasible region and enabling it to pursue performance-enhancing control strategies. To preserve the stability and recursive feasibility guarantees of the overall framework, the set $\mathcal{E}^{\mathrm{P}}$ should satisfy:

$$\mathcal{E}^{\mathrm{P}} \subseteq \mathcal{Z}^{\mathrm{C}}_{N^{\mathrm{C}}} \tag{12}$$

where $\mathcal{Z}^{\mathrm{C}}_{N^{\mathrm{C}}}$ is the N^{C}-step controllable set for the nominal component of C-MPC that steers its nominal state – within N^{C} time steps – into a terminal region $\mathcal{Z}^{\mathrm{f,C}}$, which is designed offline by tightening the actual terminal state set $\mathcal{X}^{\mathrm{f}}$ to account for the impact of the additive disturbances on the actual system.

This approach draws inspiration from applications of TMPC in passenger car systems [24] and planar quadrotor drones [27].

Remark 2. Whenever computing the maximal set $\mathcal{Z}^{\mathrm{C}}_{N^{\mathrm{C}}}$ is computationally intractable (e.g., due to complex nonlinear dynamics), a control-invariant subset, e.g., $\mathcal{Z}^{\mathrm{f,C}}$, may be used instead. Larger sets yield a larger Parent tube, where this increases the flexibility of C-MPC in exploring its search space.

As discussed in [27], designing tubes based solely on the Lipschitz constant (which in P-MPC determines the bound of the uncertainties) often leads to very large tubes and excessive conservativeness, resulting in overly tightened state constraints. While this limits the appeal of conventional TMPC schemes, as is demonstrated in Section 3, the Parent–Child MPC architecture inverts this shortcoming into an advantage, where a deliberately larger tube relaxes the constraints on C-MPC, allowing it to explore more dynamic and adaptive control strategies, ultimately resulting in improved system performance.

3.1.3. Balancing the computational overhead of P-MPC

Since the model of P-MPC is linear and its nominal optimization problem is convex (not necessarily quadratic due to the terminal constraint), P-MPC can, in view of computational costs, accommodate a larger prediction horizon than C-MPC. Larger controllable sets can be reached by sufficiently increasing the prediction horizon [4]. To reduce the computational burden of P-MPC while still enabling a large Parent prediction horizon N^{P}, two complementary strategies are proposed as outlined next.

Reduced update rate. P-MPC does not control the system, so it may be solved less frequently than C-MPC to reduce computational overhead. This requires that the updated Parent tube always covers the entire Child prediction horizon, i.e., the number of time steps between two consecutive control updates by P-MPC be strictly smaller than $N^{\mathrm{P}} - N^{\mathrm{C}} + 2$, assuming identical sampling times for both P-MPC and C-MPC.

Coarser planning sampling. Using larger sampling times, P-MPC can extend its horizon without adding more optimization variables. For stability analysis, the underlying dynamics should use the base sampling time. This can be enforced by holding control inputs constant over fixed intervals, with the associated variables and constraints removed at implementation. Prior work, e.g., [28], demonstrates how varying sampling times may significantly influence the resulting trajectories and as such the performance. This highlights the importance of careful selection of hyper-parameters, e.g., the sampling time, in hierarchical MPC design.

3.2. Child MPC

C-MPC solves a nonlinear TMPC problem to directly steer the system, optimizing the same cost function structure as P-MPC, instead of tracking its state trajectory. P-MPC shares its nominal control input trajectory and tube with C-MPC, which must ensure that its nominal state trajectory remains within the tube defined by P-MPC. By exploiting its flexibility, C-MPC discovers trajectories that enhance optimality beyond the conservative solution provided by P-MPC. The nominal optimization problem solved by C-MPC is formulated by:

$$
\begin{aligned}
V^{\mathrm{C}} \quad & \left(\boldsymbol{x}_k, \tilde{\boldsymbol{z}}^{\mathrm{P}}_{k:k+N^{\mathrm{P}}}, \tilde{\boldsymbol{v}}^{\mathrm{P}}_{k:k+N^{\mathrm{P}}-1}\right) = \\
& \min_{\substack{\tilde{\boldsymbol{z}}^{\mathrm{C}}_{k:k+N^{\mathrm{C}}}, \\ \Delta\tilde{\boldsymbol{v}}^{\mathrm{C}}_{k:k+N^{\mathrm{C}}-1}}} \left\{ \sum_{i=k}^{k+N^{\mathrm{C}}-1} \left({\boldsymbol{z}^{\mathrm{C}}_{i|k}}^{\top} Q\, \boldsymbol{z}^{\mathrm{C}}_{i|k} + {\boldsymbol{v}^{\mathrm{C}}_{i|k}}^{\top} R\, \boldsymbol{v}^{\mathrm{C}}_{i|k} \right) + \right. \\
& \left. {\boldsymbol{z}^{\mathrm{C}}_{k+N^{\mathrm{C}}|k}}^{\top} P\, \boldsymbol{z}^{\mathrm{C}}_{k+N^{\mathrm{C}}|k} \right\}
\end{aligned} \tag{13a}
$$

such that for $i = k, \dots, k + N^{\mathrm{C}} - 1$:

$$\boldsymbol{x}_k \in \left\{\boldsymbol{z}^{\mathrm{C}}_k\right\} \oplus \mathcal{E}^{\mathrm{C}} \tag{13b}$$

$$\boldsymbol{z}^{\mathrm{C}}_{i+1|k} = A\boldsymbol{z}^{\mathrm{C}}_{i|k} + g\left(\boldsymbol{z}^{\mathrm{C}}_{i|k}\right) + B\boldsymbol{v}^{\mathrm{C}}_{i|k} \tag{13c}$$

$$\boldsymbol{z}^{\mathrm{C}}_{j|k} \in \left\{\boldsymbol{z}^{\mathrm{P}}_{j|k}\right\} \oplus \mathcal{E}^{\mathrm{P}} \qquad \text{for } j = k, \dots, k + N^{\mathrm{C}} \tag{13d}$$

$$\boldsymbol{v}^{\mathrm{C}}_{i|k} = \boldsymbol{v}^{\mathrm{P}}_{i|k} + K^{\mathrm{P}}\left(\boldsymbol{x}^{\mathrm{P}}_{i|k} - \boldsymbol{z}^{\mathrm{P}}_{i|k}\right) + \Delta\boldsymbol{v}^{\mathrm{C}}_{i|k} \tag{13e}$$

$$\Delta\boldsymbol{v}^{\mathrm{C}}_{i|k} \in \left(\mathcal{V}^{\mathrm{C}} \ominus K^{\mathrm{P}}\mathcal{E}^{\mathrm{P}}\right) \ominus \left\{\boldsymbol{v}^{\mathrm{P}}_{i|k}\right\} \tag{13f}$$

This optimization is warm-started by the (virtual) solution of P-MPC, i.e., by $\tilde{\boldsymbol{z}}^{\mathrm{C}}_{k:k+N^{\mathrm{C}}} = \tilde{\boldsymbol{x}}^{\mathrm{P}}_{k:k+N^{\mathrm{C}}}$ and $\Delta\tilde{\boldsymbol{v}}^{\mathrm{C}}_{k:k+N^{\mathrm{C}}-1} = [0, \dots, 0]^{\top}$, both spanning the first N^{C} time steps. The process of generating the warm start is visualized in Fig. 1.

Constraint (13b) ensures that current nominal state $\boldsymbol{z}^{\mathrm{C}}_k$ of C-MPC, included as a decision variable, is determined such that current measured state $\boldsymbol{x}_k$ of the system is inside the tube $\left\{\boldsymbol{z}^{\mathrm{C}}_k\right\} \oplus \mathcal{E}^{\mathrm{C}}$ of C-MPC. Constraint (13c) implies that the nominal component of C-MPC operates based on the original nonlinear dynamic model (1), omitting the external disturbance $\boldsymbol{w}_k$. Thus, the tube $\mathcal{E}^{\mathrm{C}}$ of C-MPC is designed to account for rejecting these disturbances for the actual system. In essence, the Parent–Child MPC architecture allows C-MPC to avoid designing and deploying explicit terminal sets, a typically challenging task for nonlinear MPC frameworks. Instead, a sequence of tightened stage-wise state constraints, as given in (13d), which ensures that nominal state trajectory of C-MPC remains within the tube of P-MPC. These constraints, when satisfied alongside constraint (10d) within the P-MPC nominal optimization loop, ensure safe tightening of the C-MPC nominal state set, such that the actual states remain within the original admissible set $\mathcal{X}$. Constraint (13e) defines the nominal C-MPC law, where the P-MPC input (9) acts as a baseline, and C-MPC input increment $\Delta\boldsymbol{v}^{\mathrm{C}}_{i|k}$ is treated as a decision variable. Constraint (13f) ensures that the resulting C-MPC nominal inputs remain within the tightened admissible input set $\mathcal{V}^{\mathrm{C}}$. The sequence of operations performed within the Parent–Child MPC architecture is illustrated via a flowchart in Fig. 2.

In the event that $\boldsymbol{x}_k \notin \left(\mathcal{Z}^{\mathrm{C}}_{N^{\mathrm{C}}} \oplus \mathcal{E}^{\mathrm{C}}\right)$ holds, C-MPC invokes P-MPC to re-solve its optimization problem, initialized at the most recent admissible state, to re-define the Parent tube.

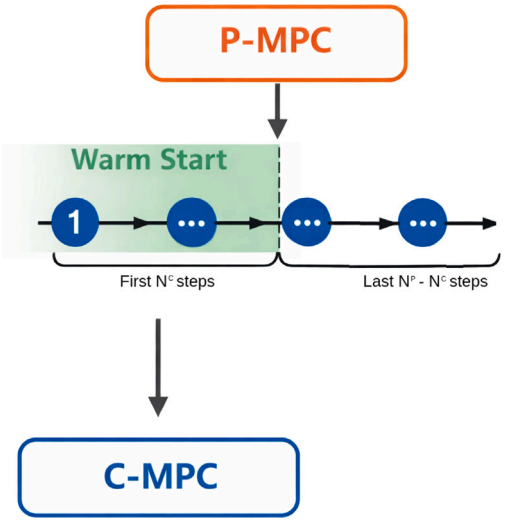

Fig. 1. The process of generating a warm start for C-MPC: The first N^{C} states and control inputs predicted by P-MPC are provided as the initial guess for C-MPC. Note that if $N^{\mathrm{C}} = N^{\mathrm{P}}$, the entire sequence generated by P-MPC is used, leaving no unused predictions.

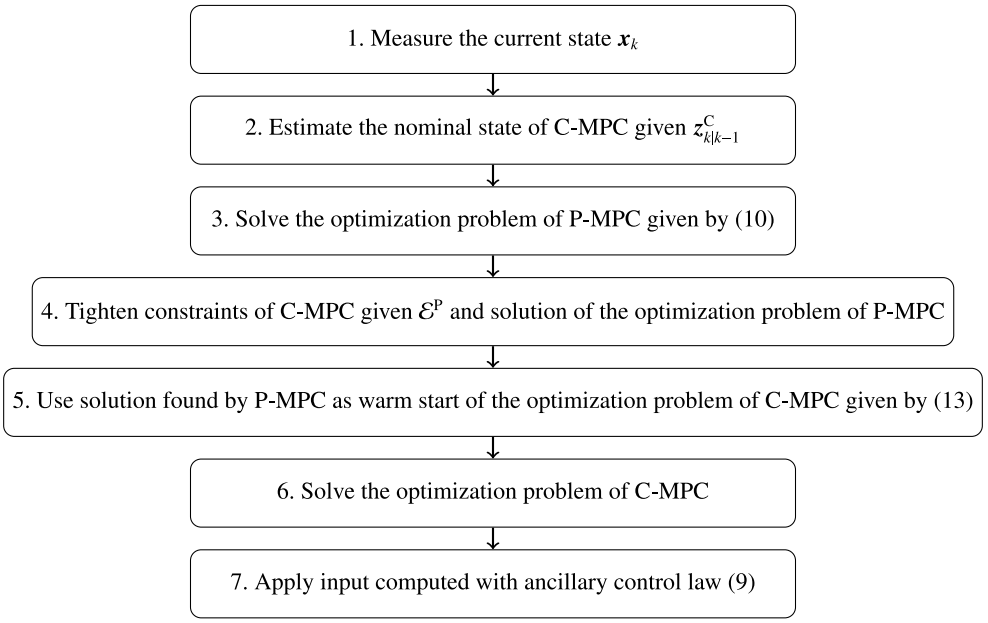

Fig. 2. Flowchart of the proposed Parent–Child MPC procedure. If P-MPC is not updated every iteration, steps 2 and 3 may be skipped.

3.3. Stability and recursive feasibility

An MPC optimization problem is recursively feasible if, whenever a solution exists for an initial state, a feasible solution also exists for all subsequent states along the resulting closed-loop trajectory [1]. A given robust positive invariant set $\mathcal{O}$ containing the origin is robustly exponentially stable for system (1), if, for all admissible disturbances $\boldsymbol{w}_k \in \mathcal{W}$, state trajectories starting within a certain bounded region converge exponentially towards set $\mathcal{O}$ [20]. The tube of P-MPC $\mathcal{E}^{\mathrm{P}}$ serves as such a robust positive invariant $\mathcal{O}$ within the architecture for the nominal trajectory of C-MPC. Thus, once the C-MPC nominal trajectory enters set $\tilde{\mathcal{Z}}^{\mathrm{C}}_{N^{\mathrm{C}}}$, a dual control strategy – such as the original TMPC formulation in (4)) – may be deployed. Accordingly, the Parent–Child MPC architecture is established, governed by(10)–(13), to be guaranteed to exponentially steer the nominal state trajectory towards set $\tilde{\mathcal{Z}}^{\mathrm{C}}_{N^{\mathrm{C}}}$. This, in turn, guarantees that the actual state trajectory reaches the actual terminal set $\mathcal{X}^{\mathrm{f}}$. To do so, it is shown that the Parent tube, which is by design a robust positive invariant set for P-MPC, also remains robustly invariant under the full Parent–Child MPC architecture. The following two theorems are proven.

Theorem 1. ***Robust invariance of the modeling error set $\mathcal{E}^P$ for C-MPC nominal state trajectory:*** *Under the Parent–Child MPC architecture, the modeling error set $\mathcal{E}^P$ – defining the cross section of the Parent tube – constitutes a robust positive invariant set for the nominal state trajectory of C-MPC.*

Proof. The stage-wise state constraint (13d) ensures that the nominal state trajectory of C-MPC remains entirely within the Parent tube, making this tube a robust positive invariant set for this trajectory. Designing the modeling error set according to (12), guarantees that the nominal P-MPC trajectory is steerable to the origin. Once this occurs, the Parent tube effectively becomes the untranslated modeling error set $\mathcal{E}^{\mathrm{P}}$. Consequently, $\mathcal{E}^{\mathrm{P}}$ itself serves as a robust positive invariant set for the nominal C-MPC trajectory, completing the proof. □

For Theorem 1 to be applicable, the nominal C-MPC problem should admit at least one feasible trajectory. The following theorem establishes the guaranteed existence of such a trajectory.

Theorem 2. ***Feasibility of the P-MPC-based warm start for nominal C-MPC:*** *The solution provided as a warm start for the C-MPC nominal problem (13) by the P-MPC layer, under the ancillary control law (9), always yields a feasible solution for nominal C-MPC—ensuring feasibility for the nominal C-MPC problem, whenever the P-MPC problem is itself feasible.*

Proof. To prove feasibility, one should show that the warm-started trajectories $\tilde{\boldsymbol{z}}^{\mathrm{C}}_{k:k+N^{\mathrm{C}}} = \tilde{\boldsymbol{x}}^{\mathrm{P}}_{k:k+N^{\mathrm{C}}}$ and $\tilde{\boldsymbol{v}}^{\mathrm{C}}_{k:k+N^{\mathrm{C}}-1} = \tilde{\boldsymbol{u}}^{\mathrm{P}}_{k:k+N^{\mathrm{C}}-1}$ satisfy all constraints of the C-MPC problem, i.e., (13b)–(13d) and (13f), assuming feasibility of the P-MPC problem and the control law given by (13e).

- **Constraint** (13b): **Tube inclusion of current state**
  - From the previous time step $k-1$, feasibility implies $\boldsymbol{x}_{k-1} \in \{\boldsymbol{z}^{\mathrm{C}}_{k-1}\} \oplus \mathcal{E}^{\mathrm{C}}$.
  - Since the tube $\mathcal{E}^{\mathrm{C}}$ of the C-MPC problem is robust positive invariant for the actual state trajectory, it follows that $\boldsymbol{x}_k \in \left\{\boldsymbol{z}^{\mathrm{C}}_{k|k-1}\right\} \oplus \mathcal{E}^{\mathrm{C}}$.
- **Constraint** (13c): **Nominal dynamics**
  - The warm-started trajectory $\tilde{\boldsymbol{z}}^{\mathrm{C}}_{k:k+N^{\mathrm{C}}} = \tilde{\boldsymbol{x}}^{\mathrm{P}}_{k:k+N^{\mathrm{C}}}$ follows the same dynamics as P-MPC.
  - Since P-MPC uses the same system model (excluding disturbances), this satisfies the nominal dynamics constraint.
- **Constraint** (13d): **Stage-wise inclusion in Parent tube**
  - By construction, the tube $\left\{\boldsymbol{z}^{\mathrm{P}}_{i|k}\right\} \oplus \mathcal{E}^{\mathrm{P}}$ of P-MPC is robust positive invariant and contains all actual P-MPC states, which in other words means the tube includes the warm-started Child trajectory.
- **Constraint** (13f): **Control input admissibility**
  - Based on (10), for the P-MPC problem $\boldsymbol{z}^{\mathrm{C}}_{k|k-1} = \boldsymbol{x}^{\mathrm{P}}_k$ holds, implying $\boldsymbol{x}_k \in \{\boldsymbol{x}^{\mathrm{P}}_k\} \oplus \mathcal{E}^{\mathrm{C}}$.
  - With the warm-started input sequence $\tilde{\boldsymbol{v}}^{\mathrm{C}}_{k:k+N^{\mathrm{C}}-1} = \tilde{\boldsymbol{u}}^{\mathrm{P}}_{k:k+N^{\mathrm{C}}-1}$, constraint (13f) boils down to the P-MPC input constraint (10e), which is satisfied by assumption of feasibility of the P-MPC problem.

□

Theorems 1 and 2 jointly establish that the Parent–Child MPC architecture guarantees the existence of at least one feasible solution that steers system (1) into a designated terminal set, thereby ensuring stabilizability.

3.4. Generalization to multi-level parent–child architecture

While a single P-MPC layer can extend the planning horizon and enhance feasibility, it may still fall short in steering the system to the terminal set — particularly in scenarios that demand large horizons and many decision variables due to complex dynamics or tight constraints. To address this, a multi-level Parent–Child MPC architecture can be adopted, where multiple P-MPC systems are stacked in a hierarchical structure. In such a recursive structure, each P-MPC serves as the Child to a higher-level Parent and itself operates as a TMPC augmented with an ancillary control law, as described in Section 3.5.2. Since each level adheres to the original design assumptions, this architecture remains theoretically valid at all depths.

As with the bi-level scheme, once the nominal state trajectory of a lower-level P-MPC enters the untranslated tube of its Parent, the top-most Parent layer is discarded, and control is delegated to the next layer. For intermediate layers, the required tube is generally larger than that used for the original C-MPC.

However, adding P-MPC layers introduces a critical trade-off: While larger Parent tubes facilitate feasibility and robustness, adding more layers increases the number of tubes where their Minkowski sum must remain within the state admissible set $\mathcal{X}$. Therefore, the design must balance warm-start feasibility, computation, and constraint satisfaction across all levels.

3.5. Special cases

Thus far, the focus has been on general implementation of the Parent–Child MPC architecture under the assumption that the original system can be stabilized via conventional tube MPC using a linear model with bounded modeling error. This section considers simpler, yet common, special cases.

3.5.1. Deterministic MPC

A widely studied variant is the deterministic MPC problem, where the disturbance in (1) is assumed to be zero. In this case, C-MPC becomes a standard deterministic MPC and solves the following deterministic optimization problem:

$$V^{\mathrm{C}}(\boldsymbol{x}_k) = \min_{\tilde{\boldsymbol{x}}_{k+1:k+N^{\mathrm{C}}}, \Delta\tilde{\boldsymbol{u}}_{k:k+N^{\mathrm{C}}-1}} \left\{ \sum_{i=k}^{k+N^{\mathrm{C}}-1} \left(\boldsymbol{x}_i^{\top} Q \boldsymbol{x}_i + \boldsymbol{u}_i^{\top} R \boldsymbol{u}_i\right) + \boldsymbol{x}_{k+N^{\mathrm{C}}|k}^{\top} P \, \boldsymbol{x}_{k+N^{\mathrm{C}}|k}^{\top} \right\} \tag{14a}$$

such that for $i = k, \dots, k + N^{\mathrm{C}} - 1$:

$$\boldsymbol{x}_{i+1|k} = A\boldsymbol{x}_{i|k} + g(\boldsymbol{x}_{i|k}) + B\boldsymbol{u}_{i|k} \tag{14b}$$

$$\boldsymbol{x}_{i+1|k} \in \left\{ \boldsymbol{z}^{\mathrm{P}}_{i+1|k} \right\} \oplus \mathcal{E}^{\mathrm{P}} \tag{14c}$$

$$\boldsymbol{u}_{i|k} = \boldsymbol{u}^{\mathrm{P}}_{i|k} + \Delta\boldsymbol{u}_{i|k} \tag{14d}$$

$$\boldsymbol{u}_{i|k} \in \mathcal{U} \tag{14e}$$

The formulation of P-MPC remains unchanged, except for constraints (10d) and (10e), which will not involve any disturbance-driven error set (i.e., $\boldsymbol{z}^{\mathrm{P}}_{i+1} \in \mathcal{X} \ominus \mathcal{E}^{\mathrm{P}}$ and $\boldsymbol{v}^{\mathrm{P}}_i \in \mathcal{U} \ominus K\mathcal{E}^{\mathrm{P}}$ for $i = k, \dots, k + N^{\mathrm{P}} - 1$). Finally, in the second phase, when the actual state enters $\mathcal{Z}^{\mathrm{C}}_{N^{\mathrm{C}}}$, a deterministic MPC controller replaces the Parent–Child MPC architecture.

3.5.2. Linear TMPC

Even without disturbances and modeling errors, the MPC problem can become computationally challenging when the number of decision variables or constraints is large, causing solvers to fails within limited time budgets. In such cases, the Parent–Child MPC architecture offers value. Since both Parent and Child components share the same system model, P-MPC can operate with a larger horizon and/or smaller sampling time, effectively planning further ahead, especially when the P-MPC optimization does not need to be solved every iteration. Despite the absence of modeling error, a Parent tube with cross section $\mathcal{E}^{\mathrm{P}}$ is designed as a positive invariant set (rather than a robust one), as well as an ancillary control law that establishes the positive invariance of $\mathcal{E}^{\mathrm{P}}$. Using solvers for convex or quadratic programs ensures computational tractability of C-MPC.

4. Case studies

This section presents two numerical case studies designed to demonstrate the performance of the Parent–Child MPC architecture. The first case study highlights its advantage over standard TMPC in linear systems, particularly in terms of feasibility and robustness. The second case study shows how this architecture can restore feasibility in a nonlinear control scenario, where standard TMPC fails due to reachability limitations.

- **Case study 1:** A Parent–Child MPC architecture is implemented for a linear system showcasing its ability to maintain robustness against disturbances while improving feasibility and reducing conservativeness compared to standard TMPC (The code is published in [29]).
- **Case study 2:** Based on the nonlinear TMPC formulation in [23], this case modifies the problem such that the original TMPC becomes infeasible due to a restrictive terminal constraint. The Parent–Child MPC architecture is then introduced to extend the reachability set and to recover feasibility (The code is provided in [30]).

All simulations were conducted on a single computer equipped with an Intel Core i9-13900HX CPU, 16 GB of RAM and an NVIDIA GeForce RTX 4070 GPU.

Case study 1: Linear system. A discrete-time double integrator system is considered with an additive disturbance, given by:

$$\boldsymbol{x}_{k+1} = \begin{bmatrix} 1 & 1 \\ 0 & 1 \end{bmatrix} \boldsymbol{x}_k + \begin{bmatrix} 0 \\ 1 \end{bmatrix} u_k + \boldsymbol{w}_k \tag{15}$$

This system models a simple kinematic scenario, with the state vector including position and velocity, and the control input corresponding to acceleration. The control objective is to steer the system from the initial state $\boldsymbol{x}_0 = [2700, 0]^{\top}$ towards the origin, minimizing cost function:

$$l(\tilde{\boldsymbol{x}}_{0:T^{\mathrm{s}}}, \tilde{u}_{0:T^{\mathrm{s}}}) = \sum_{i=0}^{T^{\mathrm{s}}} \left(\boldsymbol{x}_i^{\top} \boldsymbol{x}_i + u_i^2\right) \tag{16}$$

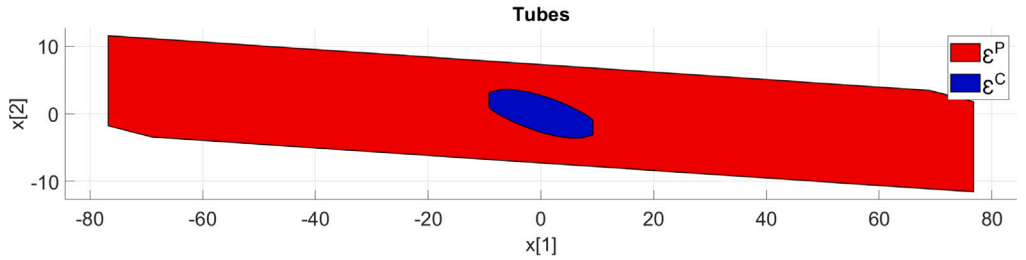

Fig. 3. Cross section of the disturbance-aware tube used by C-MPC (the same as TMPC) and P-MPC.

where T^s is the simulation time. The system is subject to constraints $-50 \leq \boldsymbol{x}[1] \leq 10000$, $|\boldsymbol{x}[2]| \leq 10000$, $|u| \leq 5$, where $[i]$ is used to show element i of a vector. The disturbance vector $\boldsymbol{w}_k$ is unknown and bounded $|\boldsymbol{w}_k| \leq 1$ for all integer values of k.

The following controllers are implemented for comparison:

TMPC: The simplest controller satisfying the design requirements is a standard linear TMPC, as described in [20], which outlines conditions for the existence of both the terminal set and the tube. The tube is computed via the method in [26] with the ancillary control law (9), using the gain $K^P = [0.2054, 0.7835]$, obtained by minimizing the following cost function:

$$l(\tilde{\boldsymbol{z}}_{0:T^s}, \tilde{v}_{0:T^s}) = \sum_{i=0}^{T^s} \left(\boldsymbol{z}_i^\top \boldsymbol{z}_i + 10 v_i^2\right) \tag{17}$$

This cost function penalizes the input more heavily (i.e., by factor 10) than the original cost in (16). This prevents overly aggressive control that will potentially violate input constraints due to excessive demand from the ancillary controller. The corresponding tube cross section is shown in Fig. 3. After constraint tightening, the admissible bounds become $-40.77 \leq \boldsymbol{z}_k[1] \leq 99990.77$, $|\boldsymbol{z}_k| \leq 9996.41$, and $|v_k| \leq 2.86$ for all non-negative integer values k. The MPT3 toolbox [31] is used to compute the terminal set, which should be symmetric about the origin. Since the tightened constraint on $\boldsymbol{z}_k[1]$ is asymmetric, it is limited further to its smaller bound, i.e., $|\boldsymbol{z}_k[1]| \leq 40.77$, when designing the terminal set. The terminal cost matrix in (4a) is set to $P = \begin{bmatrix} 2.94 & 2.36 \\ 2.36 & 4.36 \end{bmatrix}$. TMPC uses a horizon of 60.

Bi-level Parent–Child MPC: Prior to reaching $\mathcal{E}^P$, nominal C-MPC uses stage-wise constraints derived by P-MPC. P-MPC is designed to guide the system towards the target state $[40, 0]^\top$, using the following cost function:

$$l(\tilde{z}^P_{0:T^s}, \tilde{v}^P_{0:T^s}) = \sum_{i=0}^{T^s} \left((\boldsymbol{z}_i^{P\top} - [40, 0])(\boldsymbol{z}_i^P - [40, 0]^\top) + (v_i^P)^2 \right) \tag{18}$$

Targeting $[40, 0]^\top$ instead of the origin allows for a larger terminal set $\mathcal{Z}^{f,P}$ and tube cross section $\mathcal{E}^P$, delegating the goal of reaching the origin to C-MPC (or conventional TMPC in the second control phase). Upon entering $\mathcal{E}^P$, conventional TMPC is applied with a reduced prediction horizon 10. Since the system is linear and disturbance-free at the Parent level, the MPT3 toolbox may be used to compute both the tube cross section and the terminal set. To create the terminal set, the Parent ancillary control law is used with gain matrix $K^{f,P} = [0.0057, 0.11]$, obtained by solving a feedback design problem with a significantly larger input penalty ($\times 10000$) — allowing to increase the tube size (see Fig. 3).

After tightening, the bounds become $36 \leq \boldsymbol{z}_k^P[1] \leq 99914$, $|\boldsymbol{z}_k^P[2]| \leq 9984.86$, and $|v_k^P| \leq 2$ for all non-negative integers k. To reduce the number of decision variables, the same input is repeated every 4 time steps. The Parent prediction horizon N^P is set to 120, which results in 30 decision variables. To further reduce computation, P-MPC is re-solved every 6 time steps.

Results for case study 1. Two 60-step trajectories are simulated, one per controller. The Parent–Child MPC architecture requires 41 time steps before P-MPC became inactive. All optimization problems are solved using MATLAB's *quadprog* function [32] with the *active set* algorithm, which consistently results in largest solution speed.

Fig. 4 compares three controllable sets, showing that the Parent–Child MPC architecture offers the largest set. With zero initial velocity, this architecture successfully solves problems considering more than three times the initial distance from the origin that conventional TMPC can handle. The figure shows that $\mathcal{E}^P$ remains within the N^C-controllable set of C-MPC, ensuring stability and recursive feasibility. Conventional TMPC allows enhanced velocity freedom, while the tighter acceleration constraints of the Parent–Child MPC architecture result in earlier deceleration.

Fig. 5 shows the trajectories of states, control inputs, and cumulative costs: TMPC achieves a lower cost, with a maximum advantage of 117.43 and a final cost 3% lower than the Parent–Child MPC architecture, which, however, is significantly faster. TMPC takes an average of 8.21 ms per iteration, compared to 1.10 ms per iteration for the Parent–Child MPC architecture (or 2.73 ms during P-MPC updates). The time results remain consistent across the entire simulation, because a quadratic programming solver is used.

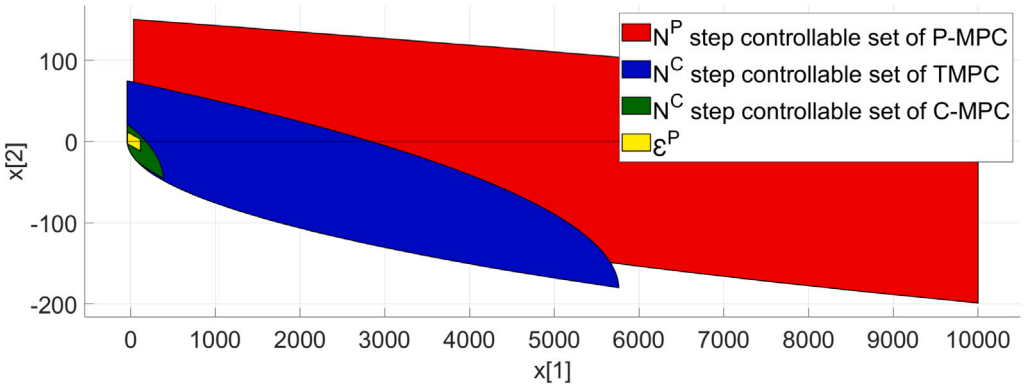

Fig. 4. Controllable sets and tube cross section for P-MPC.

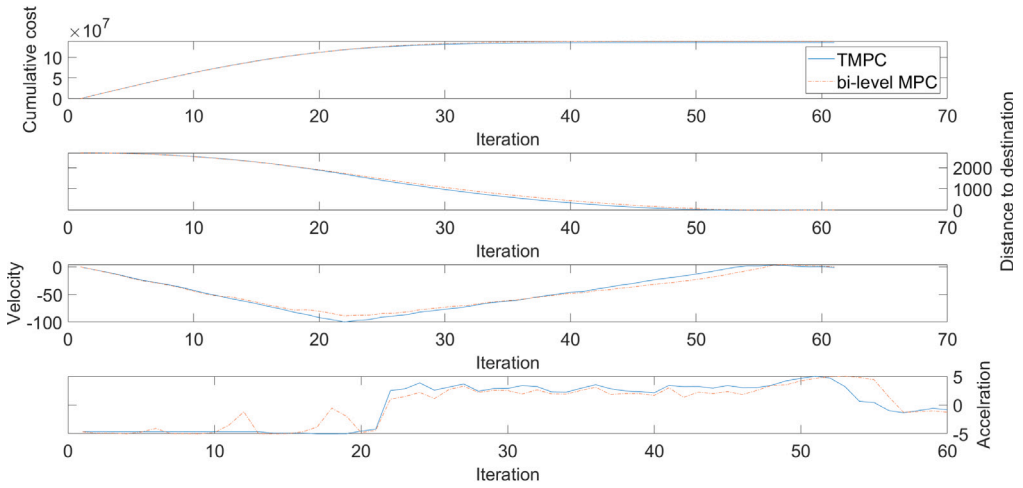

Fig. 5. Cost, state (including the position and velocity), and control input (i.e., acceleration) over time for TMPC and the Parent–Child MPC architecture.

Case study 2: Nonlinear system. In [23], a nonlinear TMPC has been proposed, employing a nonlinear ancillary control law. It has been applied to the following system:

$$\begin{bmatrix} \boldsymbol{x}_{k+1}[1] \\ \boldsymbol{x}_{k+1}[2] \end{bmatrix} = \begin{bmatrix} \boldsymbol{x}_k[2] \\ \sin\left(\boldsymbol{x}_k[1]\right) + u_k \end{bmatrix} + \boldsymbol{w}_k \tag{19}$$

The state $\boldsymbol{x}_k$ is unconstrained, while the input is limited to $|u_k| \leq 0.5$, and the disturbance satisfies $|\boldsymbol{w}_k| \leq 0.1$. The goal is to steer the system from $\boldsymbol{x}_0 = [1, 1]^\top$ towards the origin, with a terminal constraint enforcing convergence to zero.

The same system is considered, but with the input constraint tighten to $|u_k| \leq 0.3$. Under this constraint, no MPC controller can satisfy the terminal constraints within the specified horizon, resulting in infeasibility. The nominal input constraint is set to be $|v_k| \leq 0.25$ for TMPC. While extending the horizon potentially resolves this, it significantly increases computational effort and, due to non-convexity, can degrade solver performance.

A bi-level Parent–Child MPC architecture is constructed using the original TMPC as C-MPC and the following linearized model for P-MPC:

$$\boldsymbol{z}^{\mathrm{C}}_{k+1} = \begin{bmatrix} 0 & 1 \\ 0.46 & 0 \end{bmatrix} \boldsymbol{z}^{\mathrm{C}}_k + \begin{bmatrix} 0 \\ 1 \end{bmatrix} v^{\mathrm{C}}_k + \begin{bmatrix} 0 \\ g\left(\boldsymbol{z}^{\mathrm{C}}_k\right) \end{bmatrix} \tag{20}$$

where $g\left(\boldsymbol{x}_k\right) = \sin\left(\boldsymbol{x}_k[1]\right) - 0.46\boldsymbol{x}_k[1]$. To ensure validity, the state is restricted to $\left|\boldsymbol{z}^{\mathrm{C}}_k\right| \leq 4\pi/3$. These constraints do not reduce the feasibility compared to the original TMPC, which was already infeasible outside this domain. The function $g(\cdot)$ is Lipschitz and bounded, allowing us to treat it as a bounded modeling error for P-MPC, i.e., $\boldsymbol{w}^{\mathrm{P}}_k[1] = 0$ and $\left|\boldsymbol{w}^{\mathrm{P}}_k[2]\right| \leq 0.4$.

A linear ancillary control law is designed using (9) with $K^{\mathrm{P}} = [0.051, 0]$, optimized for $Q = I_{2\times 2}$ and $R = 20$. This yields a tube $\mathcal{E}$, such that $|\boldsymbol{e}^{\mathrm{P}}_k| \leq 0.68$. Consequently, the nominal input must satisfy $\left|v^{\mathrm{P}}_k\right| \leq 0.22$. The terminal set is defined as $\left|\boldsymbol{z}^{\mathrm{P}}_{k+N^{\mathrm{P}}}\right| \leq 0.68$, with a horizon of $N^{\mathrm{P}} = 10$, and a terminal cost given by ${\boldsymbol{z}^{\mathrm{P}}_{k+N^{\mathrm{P}}}}^\top \mathrm{diag}(1.15, 2.15)\boldsymbol{z}^{\mathrm{P}}_{k+N^{\mathrm{P}}}$. For C-MPC, the controller from [23] is re-used,

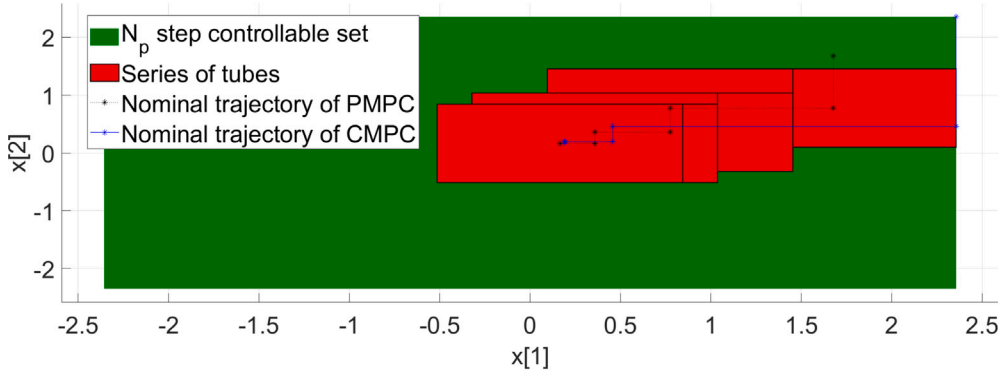

Fig. 6. The tubes, nominal states of P-MPC, and nominal states of C-MPC.

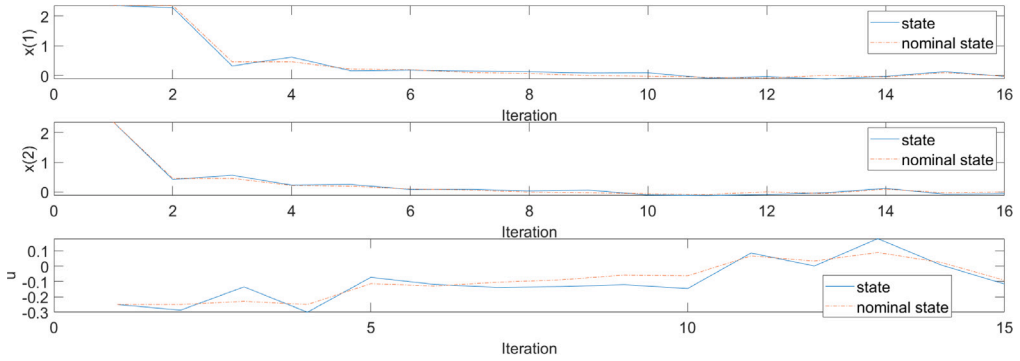

Fig. 7. Trajectory of nominal and actual states and inputs of C-MPC.

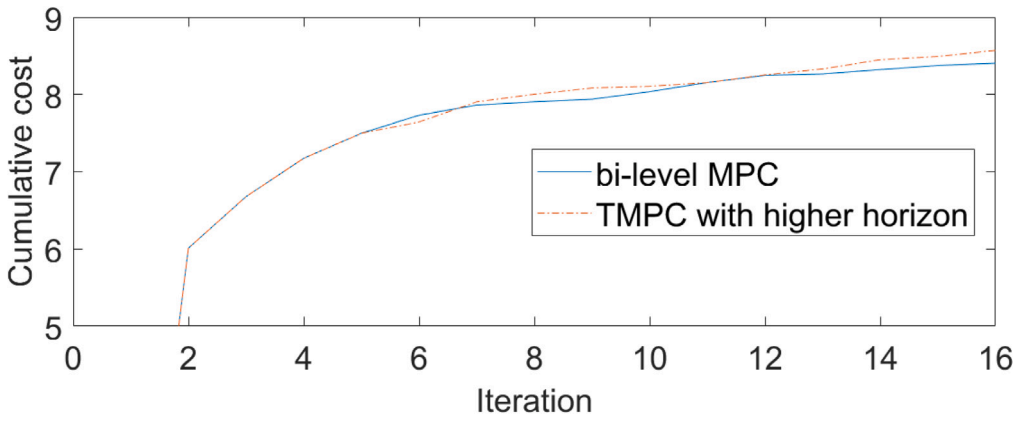

Fig. 8. Cumulative cost of the Parent–child MPC architecture and original TMPC with a larger horizon.

replacing the terminal constraint with time-varying constraints from P-MPC, as described in (13). Optimization problems are solved using *quadprog* or *fmincon* [33] with the SQP algorithm for nonlinear problems.

Results for case study 2. Both the Parent–Child MPC architecture and conventional TMPC with an extended horizon were implemented to steer the system from $\boldsymbol{x}_0 = [\pi 4/3, \pi 4/3]^\top$ towards the origin. Fig. 6 shows the tubes generated by P-MPC and the nominal trajectory determined by C-MPC, demonstrated that C-MPC successfully finds a feasible trajectory. Simulation results for the Parent–Child MPC architecture are presented in Fig. 7. Most notably, Fig. 8 compares the cumulative costs of both controllers,

Table A.1
Frequently used mathematical notations.

Abbreviation	Explanation
MPC	Model Predictive Control
TMPC	Robust tube-based Model Predictive Control
P-MPC	Parent Model Predictive Control
C-MPC	Chile Model Predictive Control

showing that they achieve comparable performance under the same cost function. Although both controllers yield similar optimal performance, their computational costs differ significantly. TMPC with an extended horizon requires an average of 7.2 ms per solve, while C-MPC takes 3.8 ms and P-MPC just 0.5 ms on average. Even though the optimization problem of C-MPC is nonlinear, the time needed to solve the problem remains consistent thanks to the warm start.

5. Conclusions and future work

This paper introduced a novel architecture, called the Parent–Child Model Predictive Control (MPC). The Parent MPC (P-MPC) layer generates long-term plans using a simplified model and/or smaller sampling times for computational efficiency and to ensure stability, while the Child MPC (C-MPC) layer refines the plan in real time to enhance performance. Formal guarantees for stability and recursive feasibility of the Parent–Child MPC architecture are provided.

The primary advantage of this architecture lies in its ability to reduce computational cost, while planning further ahead. Although C-MPC solves nonlinear, non-convex problems, the warm start from P-MPC improves the solver efficiency.

The benefits of the Parent–Child MPC architecture are demonstrated through two case studies. The first showed that this architecture reduces the computation time and expands the controllable set in linear systems. The second illustrates that – thanks to short-term corrections of C-MPC – the architecture remains effective for systems with Lipschitz nonlinearity, even though P-MPC uses an inaccurate model.

Future research should focus on applying this architecture to more complex controllers, such as state-dependent dynamic tube-based MPC [22], and to real-world systems, e.g., quadrotors [6]. Evaluating and comparing tube-generation algorithms to enhance feasibility and performance in more demanding applications are further topics for future research.

The P-MPC design assumes a low Lipschitz constant in (2). This raises the question of how small the Lipschitz constant should be. Although the literature provides examples of TMPC controllers applied under this assumption, unlike our approach, these works attempt to minimize the tube size rather than to maximize it. Consequently, they do not offer a definitive answer to the question. Future implementations should investigate the influence of larger Lipschitz constants on the P-MPC performance.

Declaration of competing interest

The authors declare the following financial interests/personal relationships which may be considered as potential competing interests: Filip Surma reports financial support was provided by Delft University of Technology. Anahita Jamshidnejad reports financial support was provided by Delft University of Technology. Filip Surma reports a relationship with Delft University of Technology that includes: employment. Anahita Jamshidnejad reports a relationship with Delft University of Technology that includes: employment and funding grants. If there are other authors, they declare that they have no known competing financial interests or personal relationships that could have appeared to influence the work reported in this paper.

Appendix A. Table of abbreviations

Abbreviations used in this paper and their corresponding explanations are given in Table A.1.

Appendix B. Table of mathematical notations

Mathematical notations frequently used in this paper and their definitions are given in Table B.2.

Data availability

The code/data has been published in 2 separate Gitlab repositories.

Table B.2
Frequently used mathematical notations.

Notation	Definition
A, B	State and input matrices in system's dynamic model
e_k^{P}	Error between nominal and actual states of P-MPC at time step k
$\mathcal{E}$, $\mathcal{E}^{\mathrm{P}}$, $\mathcal{E}^{\mathrm{C}}$	Tube cross section for, respectively, TMPC, P-MPC, and C-MPC
$g(\cdot)$, L	Function describing Lipschitz nonlinearity of the system and the Lipschitz constant, respectively
K^{P}	Feedback gain matrix for ancillary control law of P-MPC
$K^{\mathrm{f,P}}$	Feedback gain matrix for terminal control law of P-MPC
N	Prediction horizon
N^{P}, N^{C}	Prediction horizon of C-MPC and P-MPC, respectively
$l(\cdot)$	Stage cost function
P, Q, R	Terminal state, stage state, and stage input cost matrices, respectively
T^s	Simulation time
$\boldsymbol{u}_k$	Control input at time step k
$\boldsymbol{u}_k^{\mathrm{P}}$, $\boldsymbol{u}_k^{\mathrm{C}}$	Control input of, respectively, P-MPC and C-MPC, at time step k
$\mathcal{U}$	Admissible input set
$V^{\mathrm{P}}(\cdot)$, $V^{\mathrm{C}}(\cdot)$	Cost function of P-MPC and C-MPC, respectively
$\boldsymbol{v}_k$	Nominal control input at time step k
$\boldsymbol{v}_k^{\mathrm{P}}$, $\boldsymbol{v}_k^{\mathrm{C}}$	Nominal control input of, respectively, P-MPC and C-MPC at time step k
$\mathcal{V}$	Admissible nominal input set
$\mathcal{V}^{\mathrm{C}}$	Admissible nominal input set of C-MPC
$\boldsymbol{w}_k$	Disturbance vector at time step k
$\boldsymbol{w}_k^{\mathrm{P}}$	Disturbance vector of P-MPC at time step k
$\mathcal{W}$	Admissible disturbance set
$\boldsymbol{x}_k$	State vector at time step k
$\mathcal{X}$	Admissible state set
$\mathcal{X}^{\mathrm{f}}$	Terminal set
$\mathcal{X}_N$	N-step controllable set
$\boldsymbol{z}_k$	Nominal state at time step k
$\boldsymbol{z}_k^{\mathrm{P}}$, $\boldsymbol{z}_k^{\mathrm{C}}$	Nominal state of, respectively, P-MPC and C-MPC at time step k
$\mathcal{Z}_{N^{\mathrm{C}}}^{\mathrm{C}}$	N^{C}-step controllable set for the nominal component of C-MPC
$\mathcal{Z}^{\mathrm{f}}$	Nominal terminal set
$\mathcal{Z}^{\mathrm{f,P}}$	Nominal terminal set of P-MPC
$\pi(\cdot)$	Ancillary control law
$\oplus$, $\ominus$	Minkowski set summation and subtraction, respectively

References

[1] Rawlings J, Mayne D, Diehl M. Model predictive control: Theory, computation, and design. Nob Hill Publishing; 2017.
[2] Falugi P. Model predictive control: a passive scheme. IFAC Proc Vol 2014;47(3):1017–22, 19th IFAC World Congress.
[3] Chen W-H, Yan Y. New stability theory of model predictive control: modified stage cost approach. Int J Syst Sci 2025;56(4):808–26.
[4] Kerrigan E, Maciejowski J. Invariant sets for constrained nonlinear discrete-time systems with application to feasibility in model predictive control. In: Proceedings of the 39th IEEE conference on decision and control (cat. no.00CH37187). vol. 5, 2000, p. 4951–6 vol.5.
[5] Liu S, Liu J. Economic model predictive control with extended horizon. Automatica 2016;73:180–92.
[6] Chipofya M, Lee D, Chong K. Trajectory tracking and stabilization of a quadrotor using model predictive control of laguerre functions. Abstr Appl Anal 2015;2015.
[7] Zhou D, Ling KV. The effect of sample/hold time on initial feasible set in model predictive control design. In: 2013 Australian control conference. 2013, p. 212–7.
[8] Sands T. Deterministic artificial intelligence. IntechOpen; 2020.
[9] McLeland L, Erickson B, Ruchlin B, Daman E, Mejia J, Ho B, Lewis J, Mann B, Paw C, Ross J, Reis C, Walter S, Coward S, Post T, Freeborn A, Sands T. Center of mass auto-location in space for robotics. Technologies 2025;13(6):246.
[10] Kuck M, Sands T. Autonomous trajectory shaping for noise amelioration in robotics. Sensors 2024;24(2):666.
[11] Holkar K, Wagh K, Waghmare L. An overview of model predictive control. Int J Control Autom 2011;3.
[12] He D. Dual-mode nonlinear MPC via terminal control laws with free-parameters. IEEE/CAA J Autom Sin 2017;4(3):526–33.
[13] Kögel M, Ibrahim M, Kallies C, Findeisen R. Safe hierarchical model predictive control and planning for autonomous systems. Internat J Robust Nonlinear Control 2025;35:2658–76.
[14] Brdys M, Grochowski M, Gminski T, Konarczak K, Drewa M. Hierarchical predictive control of integrated wastewater treatment systems. Control Eng Pract 2008;16(6):751–67, Special Section on Large Scale Systems.
[15] Mork M, Xhonneux A, Müller D. Hierarchical model predictive control for complex building energy systems. Bauphysik 2020;42(6):306–14.
[16] Picasso B, De Vito D, Scattolini R, Colaneri P. An MPC approach to the design of two-layer hierarchical control systems. Automatica 2010;46(5):823–31.
[17] Jamshidnejad A, Sun D, Ferrara A, De Schutter B. A novel bi-level temporally-distributed MPC approach: An application to green urban mobility. Transp Res Part C: Emerg Technol 2023;156:104334.
[18] Surma F, Jamshidnejad A. Fuzzy-logic-based model predictive control: A paradigm integrating optimal and common-sense decision making. 2025, ArXiv.
[19] Tahir F. Efficient computation of robust positively invariant sets with linear state-feedback gain as a variable of optimization. In: 2010 7th international conference on electrical engineering computing science and automatic control. 2010, p. 199–204.
[20] Raković S, Mayne D. A simple tube controller for efficient robust model predictive control of constrained linear discrete time systems subject to bounded disturbances. IFAC Proc Vol 2005;38(1):241–6, 16th IFAC World Congress.
[21] Gonçalves P, Torres P, Alves C, Mondada F, Bonani M, Raemy X, Pugh J, Cianci C, Klaptocz A, Magnenat S, Zufferey J-C, Floreano D, Martinoli A. The e-puck, a robot designed for education in engineering. Proc 9th Conf Auton Robot Syst Compét 2009;1.

[22] Surma F, Jamshidnejad A. State-dependent dynamic tube MPC: A novel tube MPC method with a fuzzy model of disturbances. Internat J Robust Nonlinear Control 2025;35(4):1319–54.
[23] Mayne DQ, Kerrigan EC, van Wyk EJ, Falugi P. Tube-based robust nonlinear model predictive control. Internat J Robust Nonlinear Control 2011;21(11):1341–53.
[24] Yiqi Gao HET, Borrelli F. A tube-based robust nonlinear predictive control approach to semiautonomous ground vehicles. Veh Syst Dyn 2014;52(6):802–23.
[25] Yu S, Chen H, Allgöwer F. Tube MPC scheme based on robust control invariant set with application to Lipschitz nonlinear systems. In: 2011 50th IEEE conference on decision and control and European control conference. 2011, p. 2650–5.
[26] Rakovic S, Kerrigan E, Kouramas K, Mayne D. Invariant approximations of the minimal robust positively invariant set. IEEE Trans Autom Control 2005;50(3):406–10.
[27] Singh S, Majumdar A, Slotine J-J, Pavone M. Robust online motion planning via contraction theory and convex optimization. In: 2017 IEEE international conference on robotics and automation. 2017, p. 5883–90.
[28] Choi Y, Lee W, Kim J, Yoo J. A variable-sampling time model predictive control algorithm for improving path-tracking performance of a vehicle. Sensors 2021;21(20).
[29] Surma F. Code to test the implementation of linear Bi-level Parent-Child MPC. 4TU.ResearchData; 2025.
[30] Surma F. Code to test the implementation of nonlinear Bi-level Parent-Child MPC. 4TU.ResearchData; 2025.
[31] Herceg M, Kvasnica M, Jones C, Morari M. Multi-Parametric Toolbox 3.0. In: Proc. of the European control conference. Zürich, Switzerland; 2013, p. 502–10, http://control.ee.ethz.ch/~mpt.
[32] Mathworks. quadprog, https://www.mathworks.com/help/optim/ug/quadprog.html,
[33] Mathworks. fmincon, https://www.mathworks.com/help/optim/ug/fmincon.html.